
Contextual Memory Trees

Wen Sun

Carnegie Mellon University, Pittsburgh, PA
wensun@cs.cmu.edu

Alina Beygelzimer

Yahoo! Research, New York, NY
beygel@gmail.com

Hal Daumé III

Microsoft Research, New York, NY
University of Maryland, College Park, MD
hal@cs.umd.edu

John Langford

Microsoft Research, New York, NY
jcl@microsoft.com

Paul Mineiro

Microsoft
pmineiro@microsoft.com

Abstract

We design and study a Contextual Memory Tree (CMT), a learning *memory controller* that inserts new memories into an *experience store* of unbounded size. It is designed to efficiently query for *memories* from that store, supporting logarithmic time insertion and retrieval operations. Hence CMT can be integrated into existing statistical learning algorithms as an augmented memory unit without substantially increasing training and inference computation. We demonstrate the efficacy of CMT by augmenting existing multi-class and multi-label classification algorithms with CMT and observe statistical improvement. We also test CMT learning on several image-captioning tasks to demonstrate that it performs computationally better than a simple nearest neighbors memory system while benefitting from reward learning.

1 Introduction

When a human makes a decision or answers a question, they are able to do so while very quickly drawing upon a lifetime of remembered experiences. This ability to retrieve relevant experiences efficiently from a memory store is currently lacking in most machine learning systems (§1.1). We consider the problem of learning an efficient data structure for use as an external memory in a reward-driven environment. The key functionality of our data structure, the CMT, is the ability to *insert* new memories into a learned key-value store, and to be able to *query* those memories in the future. The storage and query functionality in the CMT is driven by an optional, user-specified, external reward signal; it organizes memories so as to maximize the downstream reward of queries. In order to scale to very large memories, our approach organizes memories in a tree structure, guaranteeing logarithmic time (in the number of memories) operations throughout (§3).

More formally, we build a datastructure, a CMT (§2), which maps *queries* (keys) to *memories* (key-value pairs). Experimentally (§4), we show this is useful in three different settings. **(a)** Few-shot learning in extreme multiclass classification problems, where the CMT is used directly as a classifier (the queries are examples and the values are class labels). Figure 1 shows that *unsupervised* CMT can statistically outperform other *supervised* logarithmic-time baselines including LOMTree [1] and Recall Tree (RT) [2] with supervision providing further improvement. **(b)** Extreme multi-label classification problems where CMT is used to augment a One-Against-All (OAA) style inference

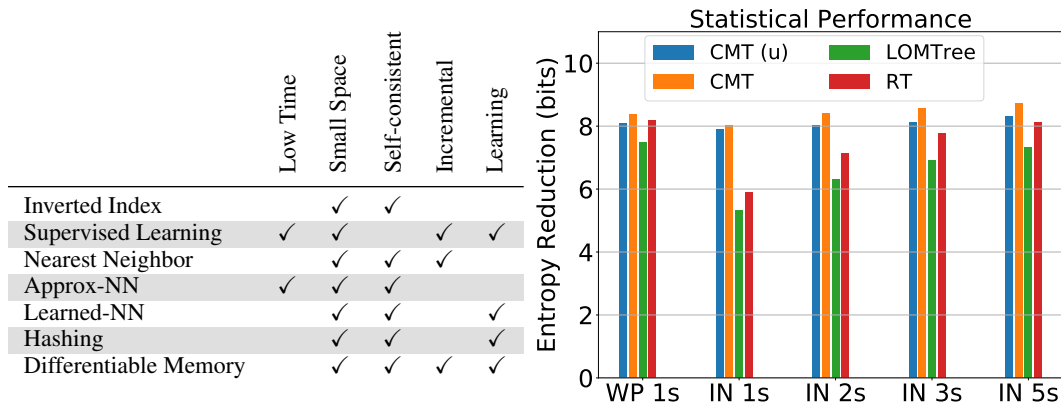


Figure 1: (Left) Desiderata satisfied by prior approaches; where answers vary with choices, we default towards ‘yes’. (Right) Statistical performance (Entropy Reduction from the constant predictor) on WikiPara one-shot (WP 1s) dataset and ImageNet S -shot datasets (IN S s) for our proposed approach (unsupervised and supervised) CMT versus baselines (LOMTree and RecallTree).

algorithm. (c) Retrieval of images based on captions, where the CMT is used similarly to a nearest-neighbor retrieval system (the queries are captions and the values are the corresponding images). External memories that persist across examples are also potentially useful as inputs to downstream applications; for instance, in natural language dialog tasks [3] and in machine translation [4], it can be useful to retrieve similar past contexts (dialogs or documents) and augment the input to the downstream system with these retrieved examples. Memory-based systems can also be useful as a component of learned reasoning systems [5, 6].

A memory $z = (x, \omega)$ is a pair of query x and value ω . The CMT operates in the following generic online manner, repeated over time:

1. Given a query x , retrieve at most k -many associated memories $\langle z_1, z_2, \dots, z_k \rangle = \text{QUERY}(x)$.
2. If rewards r_1, \dots, r_k are observed, use them to update the system via $\text{FEEDBACK}(x, \langle z_i, r_i \rangle_{i=1}^k)$.
3. If a value ω associated with x is available, INSERT a new memory $z = (x, \omega)$ into the system.

A natural goal in such a system is a notion of self-consistency. If the system inserts $z = (x, \omega)$ into the CMT, then in subsequent rounds, one should expect that (x, ω) is retrieved when $\text{Query}(x)$ is issued again for the same x . (For simplicity, we assume that all x are unique.) In order to achieve such self-consistency in a data structure that changes over time, we augment the CMT with a ‘‘Reroute’’ operation, in which the data structure gradually reorganizes itself, effectively by removing old memories and re-inserting them. We find that this Reroute operation is essential to good empirical performance (§4.1).

1.1 Existing Approaches

The most standard associative memory system is a standard map data structure (e.g., hashmap, binary tree, relational database); unfortunately, these do not *generalize* across inputs—either an input is found exactly or it is not. We are interested in memories that can *generalize* beyond exact lookups, and can *learn* to do so based on past successes and failures in an *incremental*, online manner. Because we wish to scale, the *computation time* for all operations must be at most logarithmic in the number of memories, with *constant space overhead* per key-value pair. Finally, as mentioned above, such a system should be *self-consistent*.

There are many existing approaches beyond hashmaps, all of which miss one of our desiderata (Figure 1). A basic approach for text documents is an **inverted index** [7, 8], which indexes a document by the words that appear therein. On the other end of the spectrum, **supervised learning** provides a mechanism to compile a large amount of experience into a predictor which may offer very fast evaluation, but generally cannot explicitly query for past examples.

There are several variants of nearest neighbor approaches: **a) Exact nearest neighbor** algorithms (including memory systems that use them [9]) are computationally inefficient except in special cases

```

datatype NODE =
  LEAF NODE {
    parent : NODE,
    mem : MEMORIES }
| INTERNAL NODE {
  parent : NODE,
  left, right : NODE,
  g :  $\mathcal{X} \rightarrow \{-1, 1\}$  (learning router),
  n : count of memories below }

structure CONTEXTUAL MEMORY TREE {
  root : TREE
  f : learning scorer
  M : hashmap from  $x$  to the leaf holding  $x$ 
   $\alpha \in (0, 1]$  : balance parameter
  c : multiplier on the maximum leaf size
  d : number of Reroute operations per insert

```

Figure 2: Data structures for internal and leaf nodes (left) and the full contextual memory tree (right).

[10, 11] and do not learn. **b) Approximate Nearest Neighbors** via Locality-Sensitive Hashing [12] and MIPS [13] address the problem of computational time, but not learning. **c) Nearest Neighbors with Learned Metrics** [14] can learn, but are computationally burdensome and lose incrementality.

Many of these shortcomings are addressed by **learned hashing**-based models [15, 16], which learn a hash function that works well at prediction time, but all current approaches are non-incremental and require substantial training-time overhead. Finally, **differentiable memory systems** [5, 6] are able to refine memories over time, but, relying on gradient-descent-based techniques which incur a computational overhead that is inherently linear in the number of memories.

2 The Contextual Memory Tree

At a high level, CMT is a near-balanced binary tree whose size dynamically increases as more memories are inserted. All memories are stored in leaf nodes with each leaf containing logarithmically many memories, e.g., $c \log(N)$, where N is the total number of memories and c is a constant independent of N .

Learning happens at every node of CMT. Each internal node contains a learning router. Given a query, CMT routes from the root to a leaf based on left-or-right decisions made by the routers along the way. Each internal node optimizes a metric, which ensures both its router’s ability to predict which sub-tree contains the best memory corresponding to the query, and the balance between its left and right subtrees. CMT also contains a global learning scorer that predicts the reward of a memory for a query. The scorer is used at a leaf to decide which memories to return, with updates based on an external reward signal of memory quality.

The rest of the section gives a detailed description of the data structure and the algorithms.

2.1 Data Structures

A *memory* consists of a *query* (key) $x \in \mathcal{X}$ and its associated *value* $\omega \in \Omega$. We use z to denote the memory pair (x, ω) and define $\mathcal{Z} = \mathcal{X} \times \Omega$ as the set of z . Given a memory z , we use $z.x$ and $z.\omega$ to represent the query and the value of z respectively. For instance, for multiclass classification, x is a feature vector and ω is a label. Our memory store is organized into a binary tree. A *leaf* node in Figure 2 (left top) consists of a parent and a set of memories. Leaf nodes are connected by internal nodes as in Figure 2 (left, bottom). An internal node has a parent and two children, which may be either leaf or internal nodes, a count n of the number of memories beneath the node, and a learning router $g : \mathcal{X} \rightarrow \{-1, 1\}$ which both routes via $g(x)$ and updates via $g.\text{update}(x, y)$ for $y \in \{-1, 1\}$, or $g.\text{update}(x, y, i)$ where $i \in \mathbb{R}^+$ is an importance weight of (x, y) . If $g(x) < 0$, we route x left, and otherwise right.

The contextual memory tree data structure in Figure 2 (right) has a root node, a parameter $\alpha \in [0, 1]$ which controls how balanced the tree is, a multiplier c on the maximum number of memories stored in any single leaf node, and a learning scorer $f : \mathcal{X} \times \mathcal{Z} \rightarrow \mathbb{R}$. Given a query x and memory z , the learning scorer predicts the reward one would receive if z is returned as the retrieved memory for query x via $f(x, z)$. Once a reward $r \in [0, 1]$ is received for a pair of memory z and query x , the

<hr/> Algorithm 1 PATH(query x , node v) <hr/> 1: path $\leftarrow \emptyset$ 2: while v is not a leaf do 3: $a \leftarrow$ if $v.g(x) > 0$ then right else left 4: Add $(v, a, 1)$ to path 5: $v \leftarrow v.a$ 6: end while 7: return path <hr/>	<hr/> Algorithm 4 INSERT(node v , memory z , Reroute operations d) <hr/> 1: while v is not a leaf do 2: $B = \log v.\text{left}.n - \log v.\text{right}.n$ 3: $y \leftarrow \text{sign}((1 - \alpha)v.g(z.x) + \alpha B)$ 4: $v.g.\text{update}(z.x, y)$ 5: $v.n \leftarrow v.n + 1$ 6: $v \leftarrow$ if $v.g(z.x) > 0$ then $v.\text{right}$ else $v.\text{left}$ 7: end while 8: INSERTLEAF(v, z) 9: Run REROUTE d times <hr/>
<hr/> Algorithm 2 QUERY(query x , items to return k , exploration probability ϵ) <hr/> 1: path \leftarrow PATH(x , root), path = $\{(v_i, a_i, p_i)\}_{i=1}^N$ 2: $q \in_U [0, 1]$ 3: if $q \geq \epsilon$ then 4: return $(\emptyset, \text{top}_k(\text{path.leaf}, x))$ 5: else 6: Pick $i \in_U \{1, \dots, N + 1\}$ 7: if $i \leq N$ then 8: Pick $a' \in_U \{\text{right}, \text{left}\}$ 9: $l = \text{PATH}(x, v_i, a').\text{leaf}$ 10: return $((v_i, a', 1/2), \text{top}_k(l, x))$ 11: else 12: return $((\text{path.leaf}, \perp, \perp), \text{rand}_k(\text{path.leaf}, x))$ 13: end if 14: end if <hr/>	<hr/> Algorithm 5 INSERTLEAF(leaf node v , memory z) <hr/> 1: $v.\text{mem} \leftarrow v.\text{mem} \cup \{z\}$ 2: if $ v.\text{mem} > c \log(\text{root}.n)$ then 3: $v' \leftarrow$ a new internal node with two new children 4: for $z \in v.\text{mem}$ do 5: INSERT($v', z, 0$) 6: end for 7: $v \leftarrow v'$ 8: end if <hr/>
<hr/> Algorithm 3 UPDATE($(x, z, r), (v, a, p)$) <hr/> 1: if v is a leaf then 2: $f.\text{update}(x, z, r)$ 3: else 4: $\hat{r} \leftarrow \frac{r}{p}(\mathbf{1}(a = \text{right}) - \mathbf{1}(a = \text{left}))$ 5: $y \leftarrow (1 - \alpha)\hat{r} + \alpha(\log v.\text{left}.n - \log v.\text{right}.n)$ 6: $v.g.\text{update}(x, \text{sign}(y), y)$ 7: end if 8: Run REROUTE d times <hr/>	<hr/> Algorithm 6 REMOVE(x) <hr/> 1: Find $v \leftarrow M(x)$, leaf containing x 2: $v.\text{mem} \leftarrow v.\text{mem} \setminus \{x\}$ 3: while v is not root do 4: if $v.n > 0$ then 5: $v.n \leftarrow v.n - 1$ 6: $v \leftarrow v.\text{parent}$ 7: else 8: $v' =$ the other child of $v.\text{parent}$. 9: $v.\text{parent} \leftarrow v'$ 10: $v \leftarrow v'$ 11: end if 12: end while <hr/>
	<hr/> Algorithm 7 REROUTE() <hr/> 1: Sample $z \in_U M$ 2: REMOVE($z.x$) 3: INSERT(root, $z, 0$) <hr/>

learning scorer updates via $f.\text{update}(x, z, r)$ to improve its ability to predict reward. Finally, the map M maps examples to the leaf that contains them, making removal easy.

Given any node v and query x , we define a data structure path representing the path from v to a leaf: path = $\{(v_i, a_i, p_i)\}_{i=1}^N$, where $v_1 = v$, $a_i \in \{\text{left}, \text{right}\}$ is the left or right decision made at v_i , $p_i \in [0, 1]$ is the probability with which a_i was chosen. The leaf path.leaf which the path leads to is $v_N.a_N$ typically or v if v is a leaf. As we show later, the path data structure communicates to the update rule the information needed to create an unbiased update of the routers.

2.2 Algorithms

All algorithms work given a contextual memory tree T . For brevity, we drop T when referencing its fields. We use $\in_U P$ to chose uniformly at random from a set P .

Algorithm 1 (PATH) routes a query x from any node v to a leaf, returning the path traversed.

Algorithm 2 (QUERY) takes a query x as input and returns at most k memories. The parameter $\epsilon \in [0, 1]$ determines the probability of exploration during training. Algorithm 2 first deterministically routes the query x to a leaf and records the path traversed path. With probability $1 - \epsilon$, we simply return the best memories stored in path.leaf: For a query x and leaf l , we use $\text{top}_k(l, x)$ as a shorthand for the set of $\min\{k, |l.\text{mem}|\}$ memories z in $l.\text{mem}$ with the largest $f(x, z)$, breaking ties randomly. We also use $\text{rand}_k(l, x)$ for a random subset of $\min\{k, |l.\text{mem}|\}$ memories in $l.\text{mem}$.

With the remaining probability ϵ , we uniformly sample a node along path including path.leaf. If we sampled an internal node v , we choose a random action a' and call $\text{path}(x, v.a')$ to route x to a leaf. This exploration gives us a chance to discover potentially better memories stored in the other subtrees

beneath v , which allows us to improve the quality of the router at node v . We do uniform exploration at a uniformly chosen node but other schemes are possible. If we sampled `path.leaf`, we return a random set of memories stored in the leaf, in order to update and improve the learning scorer f . The shorter the path, the higher the probability that exploration happens at the leaf.

After the query operation, the DCMT may receive a reward for a returned memory. We update the router making a randomized decision, using Algorithm 3 (UPDATE). Algorithm 3 takes an (x, z, r) as input and computes an unbiased estimate of the reward difference of the left/right decision with the balance term. When randomization occurred at the leaf instead, the scorer f is updated.

The INSERT operation is given in Algorithm 4. It routes the memory z to be inserted according to the query $z.x$ from the root to a leaf using internal learning routers, updating them on descent. Once reaching a leaf node, z is added into that leaf via INSERTLEAF. The label definition on line 3 in INSERT is the same as was used in [17]. That use, however, was for a different problem (conditional label estimation) and in different way (controlling the routing of examples rather than just advising a learning algorithm). As a consequence, the proofs of correctness given in section 3.1 differ.

When the number of memories stored in any leaf exceeds the log of the total number of memories, a leaf is split according to Algorithm 5 (INSERTLEAF). The leaf node v is promoted to an internal node with two leaf children and a binary classifier g with all memories inserted at v .

Because updates are online, they may result in a lack of self-consistency for previous insertions. This is fixed by REROUTE (Algorithm 7) on an amortized basis. Specifically, after every INSERT operation we call REROUTE, which randomly samples an example from all the examples stored in the tree, extracts the sampled example from the tree, and then re-inserts it. This relies on the REMOVE (Algorithm 6) operation, which finds the location of memory using the hashmap then ascends to the parent cleaning up accounting. When a leaf node ends up with zero memories, it is removed.

3 Properties

There are five properties that we want CMT to satisfy simultaneously (see Figure 1 (left) for the five properties). Storage (in appendix A.1) and Incrementality (in appendix A.2) are easy observations.

Appendix A.6 shows that in the limit of many REROUTES, self-consistency (defined below) is achieved.

Definition 3.1 A CMT is **self-consistent** if for all z with a unique $z.x$, $z = \text{QUERY}(z.x, 1, 0)$.

Appendix A.7 shows a learning property: At every internal node, the reward based-update rule asymptotically optimizes to a local maxima of

$$\arg \max_g E_{x \sim D} (1 - \alpha) r_{g(x)} - \alpha \log \Pr_{x \sim D} [g(x) = a], \quad (1)$$

where D is the distribution of queries induced at the node by the underlying distribution of queries at the root and the routers on the path to the root.

This leaves only logarithmic computational time, which we address next.

3.1 Computational Time

Computational time analysis naturally breaks into two parts, partition quality at the nodes and the time complexity given good partitions. To connect the two, we first define partition quality.

Definition 3.2 A K -**balanced partition** of any set has each element of the partition containing at least a $1/K$ fraction of the original set.

When partitioning into two sets, $K \geq 2$ is required. Smaller K result in smaller computational complexities at the cost of worse predictive performance in practice.

Define the progressive training error of a learning router g after seeing T examples x_1, \dots, x_T as $p = \frac{1}{T} \sum_{t=1}^T \mathbf{1}[g(x_t) \neq y_t]$, where y_t is the label assigned in line 3 of INSERT, and $g(x_t)$ is evaluated immediately after calling $g.\text{update}(x_t, y_t)$ so a mistake occurs when $g(x_t)$ disagrees with y_t after the update. The next theorem proves a bound on the partition created at an internal node, as a function of the progressive training error of the node's router and α .

Theorem 3.3 (*Partition bound*) *At any point, a router with a progressive training error of p creates a $a \frac{1 + \exp(\frac{1-\alpha}{\alpha})}{(1-p) - (1 + \exp(\frac{1-\alpha}{\alpha}))^{\frac{1}{T}}}$ -balanced partition.*

The proof is in appendix A.3, followed by a bound on the depth of K -partition trees in appendix A.4. As long as $(1-p) > \exp(\frac{1-\alpha}{\alpha})^{\frac{1}{T}}$ holds, Theorem 3.3 provides a nontrivial bound on partition. Examining limits, when $p = 0$, $\alpha = 1$ and $T = \infty$, we have $K = 2$, which means CMT becomes a perfect balanced binary tree. If $p = 0.5$ (e.g., g performs random guess), $\alpha = 0.9$ (the number of we used across all experiments) and $T = \infty$, we have $K \leq 4.3$. For any fixed T , a smaller progressive error p and a larger α lead to a smaller K .

Next, we prove that K controls the computational time.

Theorem 3.4 (*Computational Time*) *If every router g in a CMT with T previous calls to INSERT creates a K -partition, the worst case computation is $O(d(K+c) \log T)$ for INSERT, $O((K+c) \log T)$ for QUERY, and $O(1)$ for UPDATE if all stated operations are atomic.*

The proof is in appendix A.5. This theorem establishes logarithmic time computation given that K -partitions are created. The combination of these two theorems implies that the computation is logarithmic time for all nontrivial training algorithms.

4 Experiments

In this section, we study CMT empirically:

1. We apply CMT directly as an inference algorithm for few-shot multi-class classification, exploring the impact of algorithm design decisions and hyperparameter settings.
2. We combine CMT with an external inference algorithm for multi-label classification, yielding both statistical and computational benefit.
3. We use an image retrieval task to compare CMT with a simple Nearest Neighbors (NN) memory system.

Implementations of CMT and scripts for reproducing experimental results are available at (url will be provided here in final version).

To show the ability to perform incremental learning, we always train CMT in an online fashion, making multiple passes over the dataset. To test the generalization ability of CMT, we always test it on a separate test set. Overall, we find that CMT outperforms other logarithmic-time baselines on few-shot multi-class classification statistically, can potentially increase statistical and computational performance of One-Against-All (OAA) when augmenting OAA for multi-label classification, and can outperform NN both statistically and computationally, indicating the benefit of learned memories.

4.1 Ablation Analysis on Extreme Multiclass Classification

We first conduct experiments to study CMT in the context of multi-class classification, where it operates directly as an inference algorithm. A memory z is a feature vector x and label ω . Given a query x CMT returns a memory z , and receives a reward signal $\mathbf{1}(z.\omega = \omega)$. Finally the ground truth label ω is revealed and CMT inserts (x, ω) and updates.

We test the self-consistency property on the WikiPara one-shot dataset that has only one training example per class (see Figure 3a). We ran CMT in an unsupervised fashion, by only calling INSERT and using $-\|x - z.x\|$ as $f(x, z)$ to select memories at leafs. We report the self-consistency error with respect to the number of REROUTE calls per insertion (parameter d) after four passes over the dataset (tuned using a holdout set). As d increases, the self-consistency error rapidly drops.

To show that UPDATE is beneficial, we use multiple passes to drive the training error down to nearly zero. Figure 3b shows the training error versus the number of passes on the WikiPara one-shot dataset (on the x -axis, we plot the number of additional passes over the dataset, with zero corresponding to a single pass). Note that the training error is essentially equal to the self-consistency error in WikiPara One-shot, hence we see that UPDATE further enhances self-consistency due to the extra REROUTE operations in UPDATE.

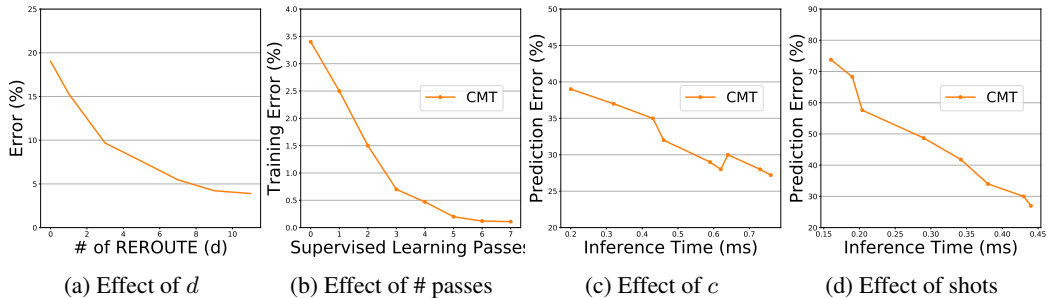


Figure 3: (a) Self-consistency of CMT with respect to the number of REROUTE operations per insertion (parameter d) on WikiPara one-shot, (b) the effect of the number of UPDATE calls on the training error on WikiPara one-shot, (c) the inference time and prediction error with respect to c on ALOI, and (d) the inference time and prediction error with respect to number of shots on ALOI.

To test the effect of the multiplier c (the leaf memories multiplier), we switch to the ALOI dataset [18], which has 100 examples per class enabling good generalization. Figure 3c shows that statistical performance improves with inference time and the value of c . In Appendix §B.2, we include plots showing statistical and inference time performance vs c in Figure 5 with inference time scaling linearly in c as expected.

Last, we test CMT on a series of progressively more difficult datasets by creating S -shot ALOI via randomly sampling S training examples per label, with S varying from 1 to 100. As ALOI has 1000 unique labels, the number of memories (i.e., training examples) CMT needs to store scales as $S \times 1000$, for S -shot ALOI. We fix $c = 4$. Figure 3d shows the statistical performance vs inference time by varying S in this test (as S increases, the inference time monotonically increases). The prediction error drops quickly as we increase S . Appendix §B.2 includes detailed plots. We observe inference time increasing logarithmically with S (Figure 6b), matching CMT’s logarithmic time operation theory.

4.2 Few-shot Multi-Class Classification

We next test CMT on few-shot multi-class classification, comparing it to two logarithmic multi-class classification algorithms, LOMTree [1], Recall Tree [2], and a linear-time One-Against-All (OAA) [19]. Here we set $k = 1$ (a parameter in QUERY, i.e., number of memories to return in a single query).

We first test CMT on the ALOI dataset. We tested both the unsupervised version (i.e., using only INSERT) and the supervised version (i.e., using INSERT for the first pass, and using UPDATE for subsequent passes). We used three passes for all algorithms. The supervised version of CMT achieved 26.3% test prediction error, outperforming LOMTree (66.7%) and Recall Tree (28.8%). The supervised version of CMT also significantly outperforms the unsupervised one (75.8%), showing the benefit of the UPDATE procedure. Since ALOI has 1000 classes, a constant predictor has prediction error larger than 99%.

We then test CMT on more challenging few-shot multi-class classification datasets, WikiPara S -shot ($S = 1, 2, 3$) and ImageNet S -shot ($S = 1, 2, 3, 5$) with only S examples per label. Such datasets make generalization extremely challenging, and hence a memory-based learning algorithm potentially has an advantage as it can remember and retrieve similar memories for prediction. Figure 1 summarizes the statistical performance (entropy reduction compared to a constant predictor) of supervised CMT, unsupervised CMT (denoted as CMT (u)), and the two logarithmic-time baselines. For one-shot experiments (WP 1-s and IN 1-s on Figure 1), CMT outperforms all baselines. The edge of CMT degrades gradually over baselines as S increases (IN S s with $S > 1$ in Figure 1). All details are included in Table 5 in Appendix §B.3.

Approach	RCV1-1K			AmazonCat-13K			Wiki10-31K		
	loss	Test time	Train time	loss	Test time	Train time	loss	Test time	Train time
CMT	2.5	1.4ms	1.9hr	3.2	1.7ms	5.3hr	18.3	25.3ms	1.3hr
OAA	2.6	0.5ms	1.3hr	3.0	8.7ms	15.5hr	20.3	327.1ms	7.2hr

Table 1: Hamming Loss, test time per example (ms), and training time (hr) for multi-label tasks.

4.3 Multi-Label Classification with an External Inference Algorithm

In this set of experiments, instead of using CMT as an inference algorithm, we integrate CMT with an external inference procedure based on One-Against-All. CMT is not aware of the external multi-label classification task, so this is an example of how an external inference algorithm can leverage the returned memories as an extra source of information to improve performance. Here each memory z consists of a feature vector x and label vector $\omega \in \{0, 1\}^M$, where M is the number of unique labels. Given a query x , its ground truth label vector ω , and a memory z , we choose the F1-score between ω and $z.\omega$ as the reward signal. We set k to $c \log(N)$ (i.e., CMT returns all memories in the leaf we reach). Given a query x , with the returned memories $\{z_1, \dots, z_k\}$, the external inference procedure extracts the unique labels from the returned memories and performs a One-Against-Some (OAS) inference [2] using the extracted labels.¹ The external system then calls UPDATE for the returned memories. Since CMT returns logarithmically many memories, we guarantee that the number of unique labels from the returned memories is also logarithmic. Hence augmenting OAS with CMT enables logarithmic inference and training time.

We compare CMT-augmented OAS with the default multi-label OAA approach (highly optimized with vectorized computation) under the Hamming loss. We compare CMT-augmented OAS to OAA on three multi-label datasets, RCV1-1K [20], AmazonCat-13K [21], and Wiki-31K [22, 23]. (The datasets are described in Table 3 in Appendix B.1.) Table 1 summarizes the performance of CMT and OAA. (LOMTree and Recall Tree are excluded because they do not operate in multi-label settings.) We see that CMT-augmented OAS achieves similar statistical performance to OAA, and even outperforms OAA on Wiki10-31K, while gaining significant computational speed up in training and inference on datasets with a large number of labels (e.g., AmazonCat-13K and Wiki10-31K). This set of experiments shows that CMT-augmented OAS can win over OAA both statistically and computationally for challenging few-shot multi-label datasets with a large number of labels.

4.4 CMT as an Image Retrieval Algorithm

Finally, we test CMT on an image retrieval task where the goal is to find an image given a caption. We used three benchmark datasets, (1) UIUC Pascal Sentence Dataset [24], (2) Flickr8k dataset [25], and (3) MS COCO [26], with feature representations described in §B.1. Here, a memory z consists of (features of) a caption x and an image ω . Given a query, CMT returns a memory $z = (x, \omega)$. Our reward function is the cosine similarity between the returned memory’s image $z.\omega$, and the ground truth image ω associated with the query x .

To show the benefit of learning in CMT, we compare it to Nearest Neighbor Search (NNS) on this task, using the Euclidean distance $\|x - z.x\|_2$ in the feature space of captions as the NNS metric.

Both CMT and NNS are tested on a separate test set, with the average reward of the retrieved memory reported. Overall, the difference in reward is negligible (on the order of 10^{-3}) and statistically insignificant. (See Appendix Table 6 for details.) However, CMT is significantly faster. Figure 4 summarizes the speedup over NNS (implemented using a linear scan). While there are NNS schemes that provide speedups over linear NNS, none guarantee logarithmic time exact retrieval without additional assumptions.

	CMT	
	unsup	sup
Pascal	5.7	1.3
Flickr8k	26.0	6.0
MSCOCO	21.0	6.5

Figure 4: Speedups over linear NNS, in (unsup)ervised and (sup)ervised mode.

¹OAS takes x and a small set of candidate labels and returns the labels with a positive score, according to a learned scoring function. After prediction, the OAS predictor receives the true labels y associated with this x and performs an update to its score function based on the true labels and the small candidate label set.

5 Conclusion

CMT provides a new tool for learning algorithm designers by enabling learning algorithms to work with either an unsupervised or reinforced logarithmic time memory store. Empirically, we find that CMT provides remarkable unsupervised performance, sometimes beating previous supervised algorithms while reinforcement provides steady improvements.

Acknowledgement

Part of this work was done when WS was at Yahoo! Research, New York. WS also thank J. Andrew Bagnell and Geoffrey J. Gordon for valuable discussion.

References

- [1] Anna E Choromanska and John Langford. Logarithmic time online multiclass prediction. In *Advances in Neural Information Processing Systems*, pages 55–63, 2015.
- [2] Hal Daume III, Nikos Karampatziakis, John Langford, and Paul Mineiro. Logarithmic time one-against-some. *ICML*, 2017.
- [3] Alexander Bartl and Gerasimos Spanakis. A retrieval-based dialogue system utilizing utterance and context embeddings. 2017.
- [4] Jiatao Gu, Yong Wang, Kyunghyun Cho, and Victor O. K. Li. Search engine guided non-parametric neural machine translation. In *AAAI*, 2018.
- [5] Jason Weston, Sumit Chopra, and Antoine Bordes. Memory networks. *CoRR*, abs/1410.3916, 2014.
- [6] Alex Graves, Greg Wayne, Malcolm Reynolds, Tim Harley, Ivo Danihelka, Agnieszka Grabska-Barwinska, Sergio Gomez Colmenarejo, Edward Grefenstette, Tiago Ramalho, John Agapiou, Adrià Puigdomènech Badia, Karl Moritz Hermann, Yori Zwols, Georg Ostrovski, Adam Cain, Helen King, Christopher Summerfield, Phil Blunsom, Koray Kavukcuoglu, and Demis Hassabis. Hybrid computing using a neural network with dynamic external memory. *Nature*, 538(7626):471–476, 2016.
- [7] Donald Ervin Knuth. *The art of computer programming, Volume I: Fundamental Algorithms, 3rd Edition*. Addison-Wesley, 1997.
- [8] Andrei Z. Broder, David Carmel, Michael Herscovici, Aya Soffer, and Jason Y. Zien. Efficient query evaluation using a two-level retrieval process. In *Proceedings of the 2003 ACM CIKM International Conference on Information and Knowledge Management, New Orleans, Louisiana, USA, November 2-8, 2003*, pages 426–434, 2003.
- [9] Lukasz Kaiser, Ofir Nachum, Aurko Roy, and Samy Bengio. Learning to remember rare events. *ICLR*, 2017.
- [10] Sanjoy Dasgupta and Kaushik Sinha. Randomized partition trees for nearest neighbor search. *Algorithmica*, 72(1):237–263, 2015.
- [11] Alina Beygelzimer, Sham Kakade, and John Langford. Cover trees for nearest neighbor. In *Machine Learning, Proceedings of the Twenty-Third International Conference (ICML 2006), Pittsburgh, Pennsylvania, USA, June 25-29, 2006*, pages 97–104, 2006.
- [12] Mayur Datar, Nicole Immorlica, Piotr Indyk, and Vahab S. Mirrokni. Locality-sensitive hashing scheme based on p-stable distributions. In *Proceedings of the 20th ACM Symposium on Computational Geometry, Brooklyn, New York, USA, June 8-11, 2004*, pages 253–262, 2004.
- [13] Anshumali Shrivastava and Ping Li. Improved asymmetric locality sensitive hashing (ALSH) for maximum inner product search (MIPS). In *Proceedings of the Thirty-First Conference on Uncertainty in Artificial Intelligence, UAI 2015, July 12-16, 2015, Amsterdam, The Netherlands*, pages 812–821, 2015.
- [14] Kilian Q. Weinberger, John Blitzer, and Lawrence K. Saul. Distance metric learning for large margin nearest neighbor classification. In *Advances in Neural Information Processing Systems 18 [Neural Information Processing Systems, NIPS 2005, December 5-8, 2005, Vancouver, British Columbia, Canada]*, pages 1473–1480, 2005.
- [15] Ruslan Salakhutdinov and Geoffrey E. Hinton. Semantic hashing. *Int. J. Approx. Reasoning*, 50(7):969–978, 2009.
- [16] Mohammad Rastegari, Ali Farhadi, and David A. Forsyth. Attribute discovery via predictable discriminative binary codes. In *Computer Vision - ECCV 2012 - 12th European Conference on Computer Vision, Florence, Italy, October 7-13, 2012, Proceedings, Part VI*, pages 876–889, 2012.

- [17] Alina Beygelzimer, John Langford, Yuri Lifshits, Gregory Sorkin, and Alex Strehl. Conditional probability tree estimation analysis and algorithms. In *Proceedings of the Twenty-Fifth Conference on Uncertainty in Artificial Intelligence*, pages 51–58. AUAI Press, 2009.
- [18] Jan-Mark Geusebroek, Gertjan J Burghouts, and Arnold WM Smeulders. The amsterdam library of object images. *International Journal of Computer Vision*, 61(1):103–112, 2005.
- [19] Ryan Rifkin and Aldebaro Klautau. In defense of one-vs-all classification. *Journal of machine learning research*, 5(Jan):101–141, 2004.
- [20] Yashoteja Prabhu and Manik Varma. Fastxml: A fast, accurate and stable tree-classifier for extreme multi-label learning. In *Proceedings of the 20th ACM SIGKDD international conference on Knowledge discovery and data mining*, pages 263–272. ACM, 2014.
- [21] Julian McAuley and Jure Leskovec. Hidden factors and hidden topics: understanding rating dimensions with review text. In *Proceedings of the 7th ACM conference on Recommender systems*, pages 165–172. ACM, 2013.
- [22] Arkaitz Zubiaga. Enhancing navigation on wikipedia with social tags. *arXiv preprint arXiv:1202.5469*, 2012.
- [23] Kush Bhatia, Himanshu Jain, Purushottam Kar, Manik Varma, and Prateek Jain. Sparse local embeddings for extreme multi-label classification. In *Advances in Neural Information Processing Systems*, pages 730–738, 2015.
- [24] Cyrus Rashtchian, Peter Young, Micah Hodosh, and Julia Hockenmaier. Collecting image annotations using amazon’s mechanical turk. In *Proceedings of the NAACL HLT 2010 Workshop on Creating Speech and Language Data with Amazon’s Mechanical Turk*, pages 139–147. Association for Computational Linguistics, 2010.
- [25] Micah Hodosh, Peter Young, and Julia Hockenmaier. Framing image description as a ranking task: Data, models and evaluation metrics. *Journal of Artificial Intelligence Research*, 47:853–899, 2013.
- [26] Tsung-Yi Lin, Michael Maire, Serge Belongie, James Hays, Pietro Perona, Deva Ramanan, Piotr Dollár, and C Lawrence Zitnick. Microsoft coco: Common objects in context. In *European conference on computer vision*, pages 740–755. Springer, 2014.
- [27] Linli Xu and Dale Schuurmans. Unsupervised and semi-supervised multi-class support vector machines. In *Proceedings, The Twentieth National Conference on Artificial Intelligence and the Seventeenth Innovative Applications of Artificial Intelligence Conference, July 9-13, 2005, Pittsburgh, Pennsylvania, USA*, pages 904–910, 2005.
- [28] Zohar Shay Karnin, Edo Liberty, Shachar Lovett, Roy Schwartz, and Omri Weinstein. Unsupervised svms: On the complexity of the furthest hyperplane problem. In *COLT 2012 - The 25th Annual Conference on Learning Theory, June 25-27, 2012, Edinburgh, Scotland*, pages 2.1–2.17, 2012.
- [29] Nicolò Cesa-Bianchi and Gábor Lugosi. *Prediction, learning, and games*. Cambridge University Press, 2006.
- [30] Yoav Freund and Robert E. Schapire. A decision-theoretic generalization of on-line learning and an application to boosting. *J. Comput. Syst. Sci.*, 55(1):119–139, 1997.
- [31] L. E. J. Brouwer. Über abbildungen von mannigfaltigkeiten. *Mathematische Annalen*, 71:97–115, 1911.
- [32] Maxime Oquab, Leon Bottou, Ivan Laptev, and Josef Sivic. Learning and transferring mid-level image representations using convolutional neural networks. In *Computer Vision and Pattern Recognition (CVPR), 2014 IEEE Conference on*, pages 1717–1724. IEEE, 2014.
- [33] Karen Simonyan and Andrew Zisserman. Very deep convolutional networks for large-scale image recognition. *arXiv preprint arXiv:1409.1556*, 2014.

A Theorems and proofs

A.1 Storage

Bounded storage is an easy desiderata to satisfy.

Claim A.1 For any $T > 0$, a contextual memory tree after T insertions requires only $O(T)$ storage.

Proof: The hashmap is $O(T)$. The number of internal nodes is bounded by the number of leaf nodes. Since every leaf node has at least one unique memory, the storage requirement for internal nodes is $O(T)$, and so is the storage requirement for the leaves. \square

A.2 Incrementality

By observation, all contextual memory tree algorithms are incremental so the overall operation is incremental as long as the underlying learning algorithms for the learning scorer and routers are incremental. In fact, the contextual memory tree is online so long as the underlying learning algorithms are online.

A.3 Partitioning

Here we prove the partition bound (theorem 3.3).

Proof: Let R_t and L_t be the number of memories in the right and left subtree respectively, at the start of round t for which we are proving the theorem.

Observe that if

$$\alpha \log \frac{L_t}{R_t} > 1 - \alpha,$$

or, equivalently, if

$$\frac{L_t}{R_t} > e^{\frac{1-\alpha}{\alpha}},$$

or equivalently, if

$$\frac{L_t}{N_t} > \frac{1}{1 + \exp(1 - \frac{1}{\alpha})}, \quad (2)$$

where $N_t = R_t + L_t$ we always have $y = 1$.

A symmetric argument shows that if

$$\frac{R_t}{N_t} > \frac{1}{1 + \exp(1 - \frac{1}{\alpha})}, \quad (3)$$

we always have $y = -1$.

Denote $\kappa = \frac{1}{1 + \exp(1 - \frac{1}{\alpha})}$. Note that $\kappa < 1$. We claim that for any t , we have

$$R_t \leq (1 - p_t)\kappa N_t + (1 - \kappa) + p_t N_t, \text{ and } L_t \leq (1 - p_t)\kappa N_t + (1 - \kappa) + p_t N_t, \quad (4)$$

where p_t is the progressive training error at the beginning of round t . We prove the claim by induction on t . The base case holds by inspection, assuming $L_2 = R_2 = 1$ and $p_2 = 0$ (i.e., by simply initializing all leaf with a default example).

Assume that the claim holds for step t , and consider step $t + 1$.

Below we first consider the first case: (1) $R_t > \kappa N_t$.

Note that in this case, we always have $y = -1$. Whether or not we route the example to the left depends on whether or not the router makes a post-update mistake. Hence, we discuss two sub-cases below.

(a) The router does not make a mistake here. In this case, the router routes the example to the left. Since no mistake happens in this round, we have $p_{t+1}N_{t+1} = p_t N_t$, i.e., the total number of mistakes remain the same. Then, we have:

$$R_{t+1} = R_t \leq (1 - p_t)\kappa N_t + (1 - \kappa) + p_t N_t \leq (1 - p_{t+1})\kappa N_{t+1} + (1 - \kappa) + p_{t+1} N_{t+1}, \quad (5)$$

where the inequality comes from the fact that $N_{t+1} = N_t + 1 > N_t$.

Now we consider the second sub-case here.

(b) The router does make a mistake. In this case, the router routes the example to the right. Note that in this case, we have $p_{t+1}N_{t+1} = p_tN_t + 1$, i.e., the total number of mistakes increases by one. Hence, we have for R_{t+1} :

$$\begin{aligned} R_{t+1} &= R_t + 1 \leq (1 - p_t)\kappa N_t + (1 - \kappa) + p_tN_t + 1 \\ &= \kappa N_t - \kappa p_t N_t + (1 - \kappa) + p_tN_t + 1 \\ &= \kappa N_t - \kappa p_{t+1}N_{t+1} + \kappa + (1 - \kappa) + p_tN_t + 1 \\ &= \kappa N_{t+1} - \kappa p_{t+1}N_{t+1} + (1 - \kappa) + p_{t+1}N_{t+1}, \end{aligned} \quad (6)$$

where the second equality uses the fact that $\kappa p_{t+1}N_{t+1} = \kappa p_tN_t + \kappa$.

With case (a) and case (b), we can conclude that for case (1) where $R_t > \kappa N_t$, we have:

$$R_{t+1} \leq (1 - p_{t+1})\kappa N_{t+1} + (1 - \kappa) + p_{t+1}N_{t+1}. \quad (7)$$

Now we consider the second case (b): $R_t \leq \kappa N_t$. In this case, regardless of where the example routes, we always have:

$$R_{t+1} \leq R_t + 1 \leq \kappa N_t + 1 = \kappa(N_{t+1} - 1) + 1 = \kappa N_{t+1} + 1 - \kappa. \quad (8)$$

Note that since $\kappa < 1$, we must have $p_{t+1}N_{t+1} \geq p_{t+1}\kappa N_{t+1}$. Hence we have

$$\begin{aligned} R_{t+1} &\leq \kappa N_{t+1} + 1 - \kappa \\ &\leq \kappa N_{t+1} + 1 - \kappa + p_{t+1}N_{t+1} - \kappa p_{t+1}N_{t+1} = (1 - p_{t+1})\kappa N_{t+1} + (1 - \kappa) + p_{t+1}N_{t+1}. \end{aligned} \quad (9)$$

With case (1) and case (2), we can conclude that for R_{t+1} , we always have:

$$R_{t+1} \leq (1 - p_{t+1})\kappa N_{t+1} + (1 - \kappa) + p_{t+1}N_{t+1}. \quad (10)$$

A symmetric argument implies

$$L_{t+1} \leq (1 - p_{t+1})\kappa N_{t+1} + (1 - \kappa) + p_{t+1}N_{t+1}. \quad (11)$$

By induction, we prove our claim.

Now given $L_t \leq (1 - p_t)\kappa N_t + (1 - \kappa) + p_tN_t$, we divide N_t on both sides to get:

$$L_t/N_t \leq (1 - p_t)\kappa + \frac{1 - \kappa}{N_t} + p_t. \quad (12)$$

Multiplying both sides by -1 and adding 1, we get:

$$\begin{aligned} 1 - L_t/N_t &= \frac{R_t}{N_t} \geq 1 - (1 - p_t)\kappa + \frac{\kappa - 1}{N_t} - p_t \\ &= (1 - p_t) - (1 - p_t)\kappa + \frac{\kappa - 1}{N_t} \\ &= (1 - p_t)(1 - \kappa) + \frac{\kappa - 1}{N_t}. \end{aligned} \quad (13)$$

As $\kappa > 0$, we get:

$$R_t/N_t \geq (1 - p_t)(1 - \kappa) - \frac{1}{N_t}. \quad (14)$$

By symmetry, we have:

$$L_t/N_t \geq (1 - p_t)(1 - \kappa) - \frac{1}{N_t}. \quad (15)$$

Substituting κ in, we get:

$$\min\{L_t/N_t, R_t/N_t\} \geq (1 - p_t) \frac{1}{\exp(\frac{1-\alpha}{\alpha}) + 1} - \frac{1}{N_t}. \quad (16)$$

□

A.4 Depth of K -partitions

Next we prove a depth bound given K -partitions.

Lemma A.2 *A tree on T points with a K -partition at every internal node has depth at most $K \log T$.*

Proof: By assumption, each internal node routes at least a $1/K$ fraction of incident points in either direction, hence at most a $1 - 1/K$ fraction of points are routed the other direction. As a consequence, at a depth d a node has at most $t(1 - 1/K)^d$ memories beneath it. The deepest internal node in the tree satisfies:

$$T(1 - 1/K)^d \geq 1$$

rearranging, we get:

$$T \geq \left(\frac{1}{1 - 1/K} \right)^d$$

Taking the log of both sides, we get:

$$\log T \geq d \log \left(\frac{1}{1 - 1/K} \right)$$

which implies

$$d \leq \frac{\log T}{\log \left(\frac{1}{1 - 1/K} \right)}.$$

Using $-\log(1 - x) \geq x$ for $0 \leq x < 1$, we get

$$d \leq K \log T.$$

□

A.5 Computational bound proof

Now we prove Theorem 3.4.

Proof: We assume that d is constant. From the depth bound, REMOVE is $O(K \log T)$. INSERTLEAF is $O(1)$ if the guard on line 2 is false. If the guard is true, then we know that $|v.m| > c \log T$ and $|v.m| - 1 \leq c \log T$ since otherwise it would have been triggered on a previous insertion. Hence, line 5 executes $O(c \log T)$ times, with each invocation of INSERT taking $O(1)$ time in this case as the while loop in line 1 is executed only once.

INSERT($\cdot, \cdot, 0$) takes $O((K + c) \log T)$ from the depth bound and the complexity of INSERTLEAF. Thus the computational complexity of REROUTE is $O((K + c) \log T)$. UPDATE takes $O(1)$ time, followed by d invocations of REROUTE, making it $O((K + c) \log T)$ time as well. INSERT(\cdot, \cdot, d) takes $O((K + c) \log T)$, followed by d invocations of REROUTE, making its total complexity $O((K + c) \log T)$.

QUERY calls PATH at most twice and then pays $O(c \log T)$ computation to find the top k memories for the query. The complexity of PATH is $O(K \log T)$, making the overall complexity of QUERY $O((K + c) \log T)$. □

A.6 Self-Consistency

Let us recall the definition of self-consistency.

Definition A.3 A CMT is **self-consistent** if for all z with a unique $z.x$, $z = \text{QUERY}(z.x, 1, 0)$.

Self-consistency holds for any z immediately after insertion under an assumption of predictor independence.

Definition A.4 Predictors are **independent predictors** if updates to one do not affect the predictions of the other. In other words, for all x , $g(x)$ only changes after $g.\text{update}()$.

Lemma A.5 If $z = \arg \max_{z'} f(z.x, z')$ and each pair of g are independent predictors, then for any contextual memory tree, INSERT(root, $z, 0$) implies $z = \text{QUERY}(z.x, 1, 0)$.

Proof: By assumption, the updates on line 4 of INSERT do not affect the value of $g(z.x)$ for nodes closer to the root. Therefore, since INSERT line 6 and PATH line 3 are identical both INSERT and QUERY walk through the same pre-existing internal nodes. At INSERTLEAF, the last execution of line 5 is for z and hence any newly created internal node also routes in the same direction. Once a leaf is reached, $z = \arg \max_{z'} f(z.x, z')$ implies the claim follows. □

Achieving self-consistency for all z simultaneously is more difficult since online updates to routers can invalidate pre-existing self-consistency. Nevertheless, the combination of the REROUTE operation and the convergence of a learning algorithms leads to asymptotic self-consistency.

Definition A.6 A **convergent learning algorithm** satisfies: \forall probability measures $D \forall$ update sequences : $\lim_{t \rightarrow \infty} \Pr_{x' \sim D}(x' : g_t(x') \neq g_{t-1}(x')) = 0$.

Restated, a convergent learning algorithm as one which disturbs fewer predictions the more updates that it gets. This property is an abstraction of many existing update rules with decaying learning rates.

Theorem A.7 *If $z = \arg \max_{z'} f(z.x, z')$, each pair of g are independent predictors, and g is a convergent learning algorithm, then in the limit as $\mathcal{T}.d \rightarrow \infty$, all contextual memory trees are self-consistent for all memories.*

Proof: The proof operates level-wise. At the root, for any x , the REROUTE operation introduces x as often as necessary. Since the learning algorithm is convergent by assumption, if we choose D uniform over the set of memories, then these updates eventually change the routing of zero memories. At this point, we are guaranteed that the decision in line 6 of INSERT is unchanged by further updates for all x simultaneously.

Once the root routes in a self-consistent fashion, the same logic applies recursively to every internal node amongst the memories routed to that internal node. Hence, we have self-consistency for the routing of all x by all g simultaneously. To finish the proof, we just use the assumption that $z = \arg \max_{z'} f(z.x, z')$. \square

Asymptotic self-consistency is a relatively weak property so we also study self-consistency empirically in section 4.1.

A.7 Learning

Finding a good partition from a learning perspective is plausibly more difficult than finding a good classifier. For example, in a vector space finding a partition with a large margin which separates input points into two sets each within a constant factor of the original in size is an obvious proxy. The best results for this problem [27, 28] do not scale to large datasets or function in an online fashion.

For any given node we have a set of incident samples which cause updates on INSERT or UPDATE. Focusing on UPDATE at a single node, the natural function to optimize is a form of balanced expected reward. If r_a and p_a are the rewards and probabilities of taking action a , then a natural objective is:

$$\arg \max_g E_{x \sim D} (1 - \alpha) r_{g(x)} - \alpha \log p_{g(x)}^g \quad (17)$$

where $p_a^g = \Pr_{x \sim D}(g(x) = a)$ is the probability that g chooses direction a as induced by samples over x . This objective both maximizes reward and minimizes the frequency of the chosen action, implying a good solution sends samples in both directions.

The performance of the partitioner is dependent on the classifier g which optimizes importance weighted binary classification. In particular, we evaluate the performance of g according to:

$$\hat{E}_{x,y,i} I(g(x) \neq y)$$

with the goal of g minimizing the empirical importance weighted loss over observed samples.

Next we prove a basic sanity check theorem about the asymptotics of learning a single node. For this theorem, we rely upon the notion of a no-regret [29] g which is also convergent. Common no-regret algorithms like Hedge [30] are also convergent for absolutely continuous D generating events. The following theorem relies on the

Theorem A.8 *For all absolutely continuous distributions D over updates with $d = 0$ reroutes and for all compact convergent no-regret g :*

$$\lim_{t \rightarrow \infty} g_t$$

exists and is a local maxima of (17).

The proof is in Appendix A.8. Here, convergent g is as defined in section A.6 and compact g refers to the standard definition of a compact space for the parameterization of g .

This theorem shows that the optimization process eventually drives to a local maxima of (17) providing a single node semantics. Since every node optimizes independently, the joint system therefore eventually achieves convergence over 1-step routing deviations.

A.8 Learning proof

Proof: Consider wlog the root node of the tree, and then apply this argument recursively.

Since g is no-regret the g minimizing (17) for any observed p eventually wins. Since the D producing updates is absolutely continuous, convergence of g implies convergence of p and the g, p system is compact since g is compact and p is compact. Given this, a g, p pair maps to a new g, p pair according to the dynamics of the learning algorithm.

Brouwer’s fixed point theorem [31] hence implies that there exists a g, p pair which is a fixed point of this process. Since g is no-regret, the system must eventually reach such a fixed point (there may be many such fixed points in general).

For a given g , let $\Phi^{(g)} = E_{x \sim D} \left[(1 - \alpha)r_{g(x)} - \alpha \log p_{g(x)}^g \right]$ be the objective in equation (17) and define

$$\begin{aligned} r_{\text{Left}}^{(g)} &= (1 - \alpha)r_{\text{Left}} - \alpha \log p_{\text{Left}}^g \\ r_{\text{Right}}^{(g)} &= (1 - \alpha)r_{\text{Right}} - \alpha \log p_{\text{Right}}^g. \end{aligned}$$

Using this definition, we can define:

$$\begin{aligned} y^{(g)} &= r_{\text{Right}}^{(g)} - r_{\text{Left}}^{(g)} \\ &= (1 - \alpha)(r_{\text{Right}} - r_{\text{Left}}) - \alpha(\log p_{\text{Right}}^g + \log p_{\text{Left}}^g) \\ &= (1 - \alpha)(r_{\text{Right}} - r_{\text{Left}}) + \alpha \log \frac{p_{\text{Left}}^g}{p_{\text{Right}}^g} \\ &\stackrel{a.s.}{=} (1 - \alpha)(r_{\text{Right}} - r_{\text{Left}}) + \alpha \lim_{\substack{t \rightarrow \infty \\ S \sim D^t}} \log \frac{\sum_{x \in S} I(g(x) = \text{Left})}{\sum_{x \in S} I(g(x) = \text{Right})}. \end{aligned}$$

Assume wlog that $r_{\text{Right}}^{(g)} > r_{\text{Left}}^{(g)}$ such that $|y^{(g)}| = y^{(g)}$. Examining Line 5 of UPDATE, for a fixed g (i.e. $g.\text{update}()$ has converged), taking expectations wrt p over a , and denoting H as the complete empirical history of the node,

$$\begin{aligned} E_p y &= (1 - \alpha) E_{a \sim \bar{p}} \left(\frac{r_{\text{Right}} I(a = \text{Right})}{p(\text{Right})} - \frac{r_{\text{Left}} I(a = \text{Left})}{p(\text{Left})} \right) + E_{x \sim D} \log \frac{\sum_{x \in H} I(g(x) = \text{Left})}{\sum_{x \in H} I(g(x) = \text{Right})} \\ &\stackrel{t \rightarrow \infty}{=} (1 - \alpha)(r_{\text{Right}} - r_{\text{Left}}) + E_{\substack{x \sim D \\ S \sim D^t}} \log \frac{\sum_{x \in S} I(g(x) = \text{Left})}{\sum_{x \in S} I(g(x) = \text{Right})}. \end{aligned}$$

In other words, $\lim_{t \rightarrow \infty} E_p y \stackrel{a.s.}{=} y^{(g)}$. The expected loss of g then converges to:

$$E \left[|y^{(g)}| I(g(x) \neq \text{sign}(y^{(g)})) \right] \stackrel{a.s.}{=} \Phi^{(g)}$$

proving the theorem. □

B Experimental Details

B.1 Datasets

dataset	task	classes	examples
ALOI	Visual Object Recognition	10^3	10^5
WikiPara (S -shot)	Language Modeling	10^4	$S \times 10^4$
ImageNet (S -shot)	Visual Object Recognition	2×10^4	$2S \times 10^4$
Pascal	Image-Caption Q&A	/	10^3
Flickr-8k	Image-Caption Q&A	/	8×10^3
MS COCO	Image-Caption Q&A	/	8×10^4

Table 2: Datasets used for experimentation on multi-class and Image Retrieval

dataset	# Training	# test	# Categories	# Features	Avg # Points/Label	Avg # Labels/Point
RCV1-2K	623847	155962	2456	47236	1218.56	4.79
AmazonCat-13K	1186239	306782	13330	203882	448.57	5.04
Wiki10-31K	14146	6616	30938	101938	8.52	18.64

Table 3: Extreme Multi-Label Classification datasets used for experimentation

Table 2 summarizes the datasets used in Multi-class classification and image retrieval experimentations. ALOI [18] is a color image collection of one-thousand small objects. We use the same train and test split and feature representation as Recall Tree [2]. The few-shot ImageNet datasets are constructed from the whole ImageNet

	# unsupervised passes	# supervised passes	c	d	α
ALOI	1	2	4	5	0.1
Few-shot WikiPara	1	1	4	5	0.9
Few-shot ImageNet	1	1	4	3	0.9
RCV1-1K	1	3	2	3	0.9
AmazonCat-13K	1	3	2	3	0.9
Wiki10-31K	1	3	2	3	0.9
Pascal	1	1	10	1	0.9
Flickr	1	1	10	1	0.9
MS COCO	1	1	10	1	0.9

Table 4: Key parameters used for CMT for our experiments

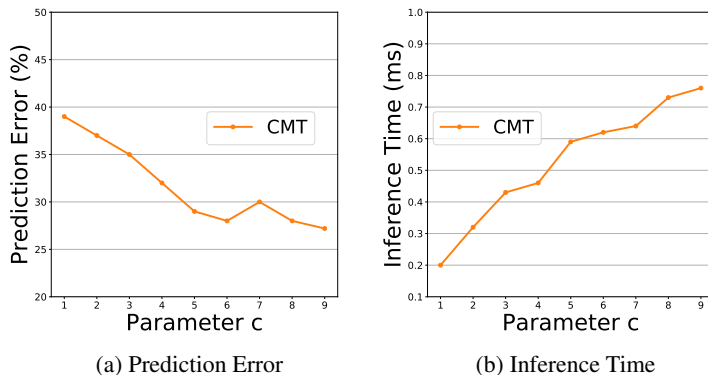


Figure 5: Performance and inference time of CMT versus the number of examples per leaf

that has 20,000 classes and 10^7 training examples. We use the same train and test split as Recall Tree [2]. The features of images are extracted from intermediate layers of a convolutional neural network trained on the ILSVRC2012 [32]. To construct a S -shot ImageNet dataset, we randomly sample S training examples for each class. A S -shot ImageNet dataset hence has a $20000 \times S$ many training examples.

Pascal sentence dataset consists of 1000 pairs of image $I \in \mathbb{R}^{300 \times 180}$ and the corresponding description of the image. We compute HoG feature y for each image I and token occurrences $y \in \mathbb{R}^{20}$ for each description using Scikit-learn’s Hashing functionality. The resulting feature x is high dimensional but extremely sparse. We randomly split the dataset into a training set consisting of 900 pairs of images and their descriptions and a test set with the remaining data. A memory $z = (x, y)$ here consists of the image feature y and the descriptions’ feature x . During inference time, given a query x (i.e., a description of an unknown image), CMT retrieves a memory $z' = (x', y')$, such that the image y' associated with the memory z' is as similar to the unknown image associated with the test query x . Given two memories z and z' , the reward signal is defined as $r(z_y, z'_y) = \langle z_y, z'_y \rangle$. The Flickr8k dataset consists of 8k images and 5 sentences descriptions for each image. Similar to Pascal, we compute HoG feature y for each image and hashing feature x for its 5-sentence description. The MS COCO image caption dataset consists of 80K images in training set, 4000 images in validation set and testing set. We extract image feature y from a fully connected layer in a VGG-19 [33] pre-trained on ILSVRC2012 dataset. We use hashing feature x for image captions.

Table 3 summarizes the datasets used for multi-label classification task. All three datasets are obtained from the Extreme Classification Repository (<http://manikvarma.org/downloads/XC/XMLRepository.html>).

All datasets that we used throughout this work are available at (url will be provided here).

B.2 Extra Plots in Sec. 4.1

Figure 5 shows the detailed plots of CMT’s statistical performance (a) and inference performance (b) with respect to parameter c (i.e., the maximum number of memories per leaf: $c \log(N)$). As shown in Figure 5 (b), the inference time increases almost linear with respect to c , which is expected as once we reach a leaf, we need to scan all memories stored in that leaf.

Figure 6 shows the detailed plots of CMT’s statistical performance (a) and inference time (b) with respect to the number of shots (i.e., number of training examples for each class) in ALOI. Note that ALOI has in total 1000

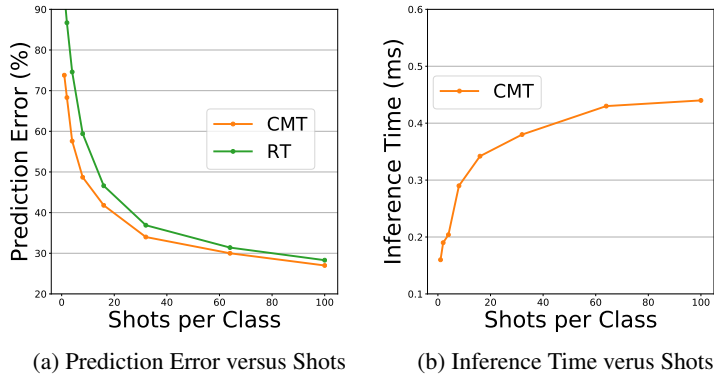


Figure 6: Performance (a) and inference time (b) of CMT versus the number of training examples per label in ALOI (i.e., shots S).

classes and hence for ALOI S -shot, we will have in total $S \times 1000$ examples. Namely as S increases, CMT has more memories to store. We vary S from 1 to 100. Figure 6a shows the performance of CMT improves quickly as S increases (e.g., dataset becomes easier to learn). Also CMT consistently outperform Recall Tree, with larger margin at fewer shots. From Figure 6 (b), we see that the inference time increases sublinearly with respect to the number of shots (i.e., the number of total memories stored in CMT), which is also expected, as we show that the depth of CMT and the number of memories per leaf are logarithmic with respect to the size of CMT.

B.3 Few-shot Extreme Multi-class Classification Details

		CMT (u)	CMT	LOMTree	Recall Tree	OAA
ALOI	Test Error	75.8	26.3	66.7	28.8	21.7
	Test Time	0.27	0.15	0.01	0.02	0.05
WikiPara (1-shot)	Test Error	97.3	96.7	98.2	97.1	98.2
	Test Time	0.3	0.3	0.1	0.1	0.9
WikiPara (2-shot)	Test Error	96.3	96.0	96.7	94.0	95.6
	Test Time	0.4	0.4	0.1	0.1	1.1
WikiPara (3-shot)	Test Error	96.1	95.7	96.1	92.0	92.8
	Test Time	0.5	0.3	0.1	0.1	1.1
ImageNet (1-shot)	Test Error	98.8	98.7	99.8	99.7	98.0
	Test Time	9.6	8.2	1.0	3.3	112.4
ImageNet (2-shot)	Test Error	98.7	98.3	99.6	99.3	97.0
	Test Time	11.7	8.6	1.2	3.3	112.0
ImageNet (3-shot)	Test Error	98.6	98.1	99.4	98.9	96.2
	Test Time	9.8	8.5	4.6	3.3	109.0
ImageNet (5-shot)	Test Error	98.4	97.9	99.2	98.6	95.3
	Test Time	12.5	11.6	1.3	4.0	110.4

Table 5: Prediction error (%) and inference time (ms) of different multi-class classification algorithms on few-shot extreme multi-class classification datasets.

Table 5 shows the detailed prediction error and inference time of CMT and other baselines. For ALOI, we briefly tuned the parameters of CMT based on a set of holdout training data, and for few-shot WikiPara (and few-shot ImageNet), we briefly tuned the parameters of CMT using the one-shot dataset on hold-out dataset and then simply just use the same set of parameters across all other few-shot datasets. The detailed key parameters can be found in Table 4.

One interesting observation from Table 5 is that CMT can outperform even OAA at the one-shot WikiPara experiment. All the datasets have same number of examples per class and hence a constant predictor (i.e., prediction by majority) would have prediction accuracy at $1/(\# \text{ of classes})$.

B.4 Multi-Label Classification

The key parameters we used to conduct our multi-label experiments are summarized in Table 4. We briefly tuned the number of supervised passes and α on holdout training datasets and picked a set of parameters that worked well for all datasets in general. We did not tune parameters c and d .

B.5 Image Retrieval

		CMT (u)	CMT	NN
Pascal	Test Reward	0.680±0.008	0.694±0.010	0.683 ±0.013
	Test Time (ms)	0.13	0.58	0.74
Flickr8k	Test Reward	0.733±0.004	0.740±0.002	0.736 ±0.003
	Test Time (ms)	0.23	1.0	6.0
MS COCO	Test Reward	0.581	0.584	0.585
	Test Time (ms)	0.590	1.90	12.4

Table 6: Performance (average reward % and time *ms*) of different approaches on image retrieval tasks.

For Pascal and Flickr8k, we randomly split the dataset into a pair of training set and test set. We create 5 random splits, and use one split for tuning parameters for CMT. For MS COCO, we use the default training, validation, and test split, and tune parameters on validation set.

For image retrieval applications, the key parameters used by CMT are summarized in Table 4, and the detailed performances of CMT and NN are summarized in Table 6. For Pascal and Flickr8k, since we have 5 training/test split, we report mean and standard deviation.

In this set of experiments, for CMT, during training we set k to be $c \log(N)$, i.e., we returned all memories stored in a single leaf to get reward signals to update f . During testing, for both CMT and NN, we report the average reward of the top returned memory on given test sets.

Table 6 summarizes the performance of CMT and NN. Note that on Pascal and Flickr8k, CMT slightly outperforms NN in terms of average reward on test sets, indicating the potential benefit of learned memories.